

## **2. Experimental techniques**

### **2.1. Introduction**

Little information is available on activity-composition relations of vanadium in contact with high  $\text{Al}_2\text{O}_3$ -CaO-MgO slags, as indicated by the previous section. Although metal droplet entrainment has been identified as one of the possible mechanisms of vanadium loss to the slag, this section will concentrate solely on the quantification of the effect of the slag basicity on soluble vanadium loss to the slag. The experimental technique involved the equilibration of synthetic CaO- $\text{Al}_2\text{O}_3$  slags with a vanadium crucible by maintaining the required oxygen activity using  $\text{H}_2$ - $\text{H}_2\text{O}$  gas mixtures. After equilibration the slags were quenched, polished and analysed using energy dispersive X-ray analysis (EDX) techniques. Knowing the mole fraction of  $\text{VO}_{1.5}$  in the slag and the mole fraction of water in the reaction gas, the vanadium activity coefficient  $\gamma_{\text{VO}_{1.5}}$  was determined for a range of CaO/ $\text{Al}_2\text{O}_3$  - ratios.

### **2.2. Experimental set-up**

#### **2.2.1. Gas system set-up**

As indicated previously, ultra-low oxygen activities based on the assumption that the oxygen activity in the industrial smelting furnace is fixed by the  $\text{Al}_2\text{O}_3/\text{Al}$ - equilibrium can only be obtained using hydrogen gas equilibrated with water vapour. The amount of water vapour was fixed by contracting hydrogen gas with 75.7 % sulphuric acid at a controlled temperature of  $42 \pm 0.1^\circ\text{C}$ . A schematic representation of the gas system is depicted in figure 24, while figure 25 shows the complete experimental set-up used in the present study.

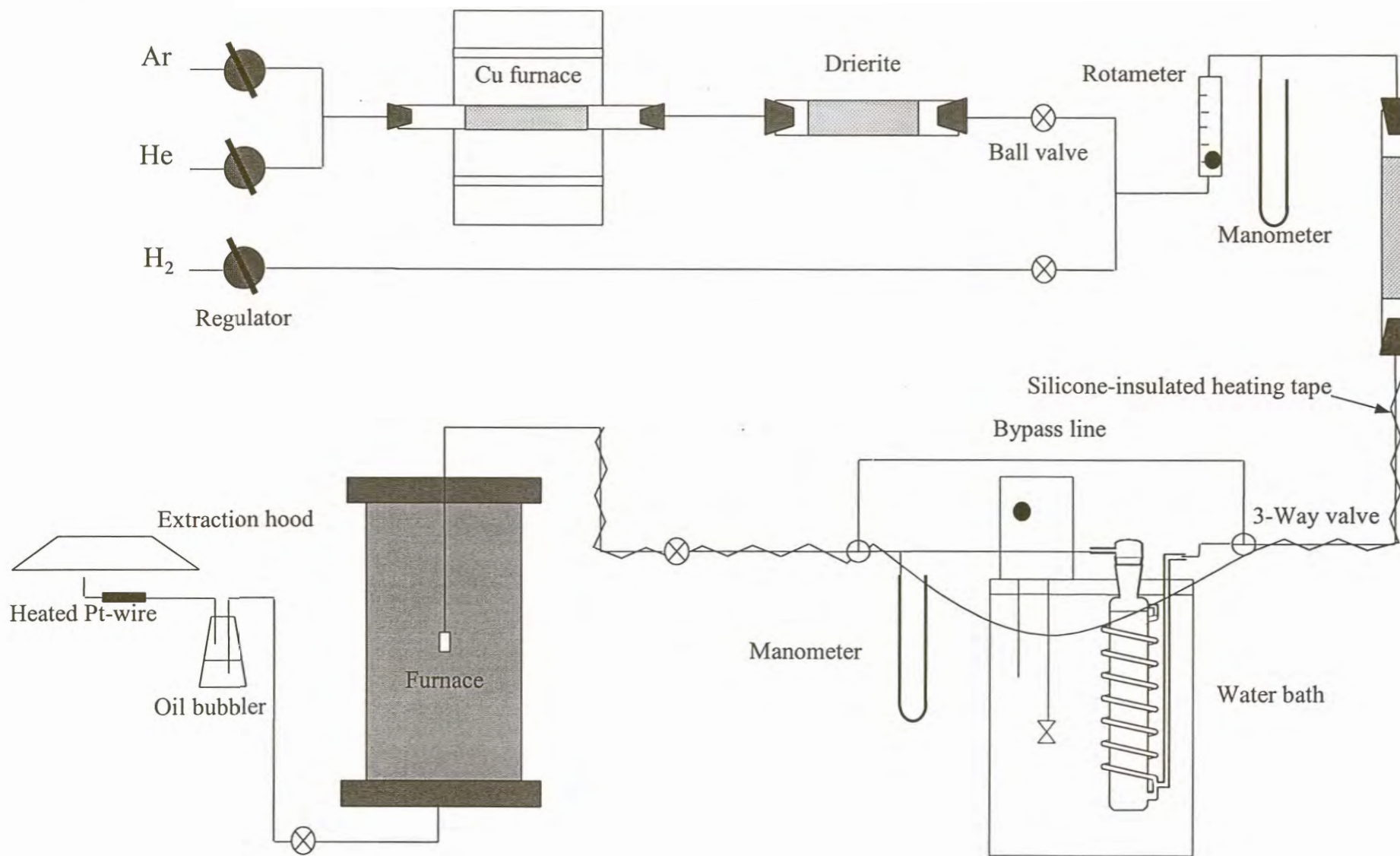


Figure 24: Schematic of gas system.

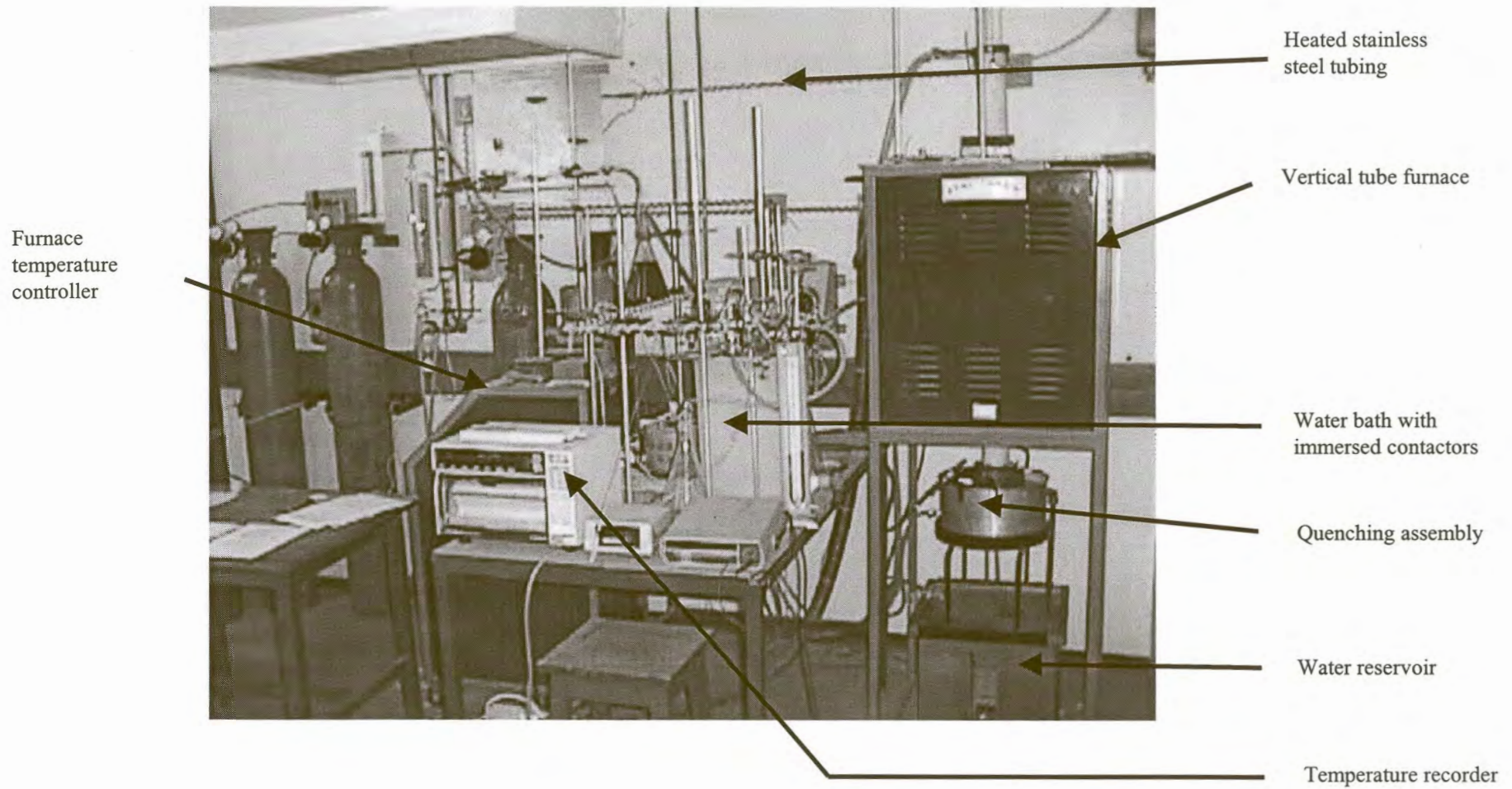


Figure 25: The complete experimental set-up used in the present study showing the gas system and furnace set-up

Tygon high-density tubing was originally used to convey the reaction gas, but difficulties in establishing a constant water vapour level led to the replacement of the tubing by stainless steel tubing. Pieces of stainless steel tubing were connected using stainless steel Swagelok couplings ensuring good tight seals. The stainless tubing (O.D. 10 mm, I.D., 8 mm) was heated to 80 °C using silicone-insulated heating tape connected to a 220 V power source. The power rating of the heating tape was 30 W/m, and 18m of heating tape was helically wound, with a 2.5 cm pitch, around the stainless steel tubing. Desorption of the absorbed water from the inner surface of the stainless steel tubing was enhanced by the continuous flushing of the tubing with Argon gas for a few days. The dryness of the tubing was monitored by passing the humid Argon stream through a Drierite-filled column, subsequently weighing the column to measure the mass increase due to water uptake as shown in figure 26.

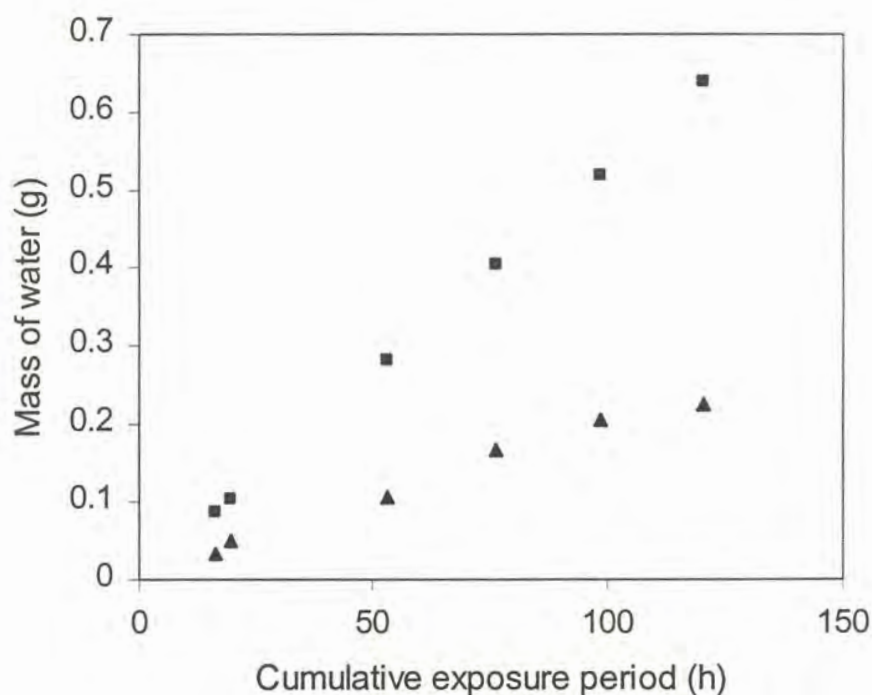


Figure 26: Humidity measurements performed on Argon gas used to convey desorbed water which originated from the walls of the stainless steel tubing. In this figure, the squares show the expected amount of water transferred for equilibrium with 85% sulphuric acid at 60 °C, and the triangles show the amount of water stripped from the tube surface if dry argon is used.

Figure 26 indicates that at least 120 hours of flushing is necessary to remove most of the absorbed water, before commencement of the equilibrium runs.

It was found that care had to be taken when weighing the Drierite-filled columns to measure the amount of water uptake, because the columns slowly changed weight over periods of tens of minutes after removal from the gas line. This effect is presumed to reflect a slightly higher pressure within the porous bed in the columns. As the gas flows out of the pores and exchange occurs between the gas inside the column with air (which has a different density), the column mass decreases, as illustrated by figure 27.

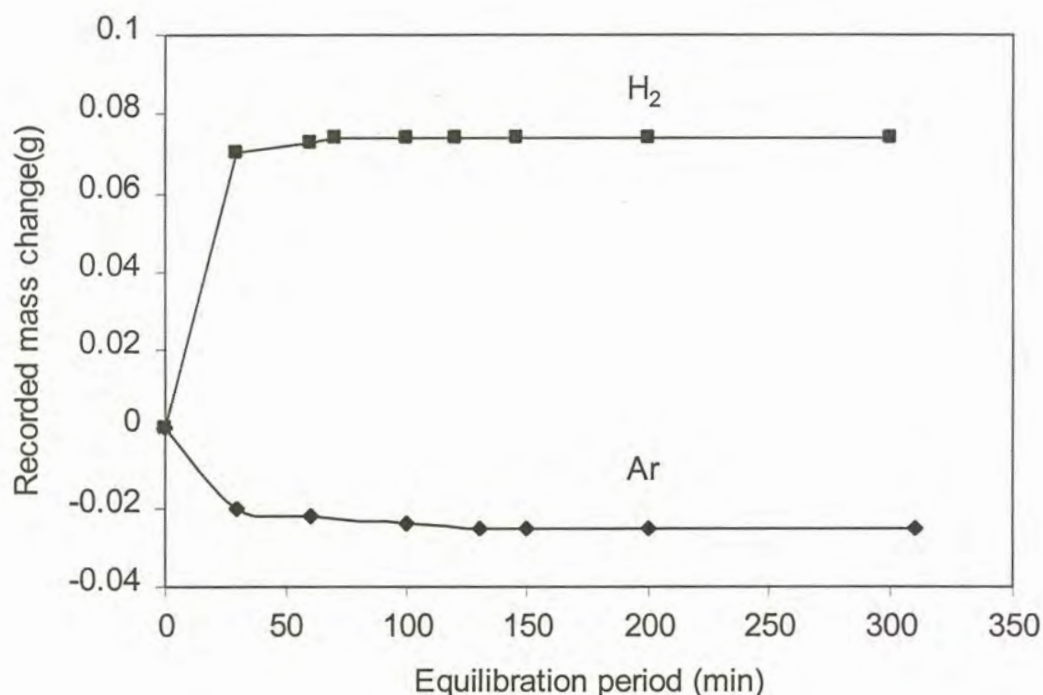


Figure 27: Change in the weight of two Drierite-filled columns containing argon and hydrogen carrier gases, after removal from the gas line.

Figure 27 serves to illustrate the required equilibration period for the two *Drierite*-filled columns, for the two different carrier gases. This figure reveals that at least 130 minutes should be allowed for the argon-filled column to equilibrate (after removal from the gas line), compared to the 70 minutes for the hydrogen-filled column. The Argon-filled column shows a net weighed decrease while the hydrogen filled-column increased. The equilibration period for argon-filled columns was throughout the moisture measurements

much shorter compared to instances when hydrogen was used. Argon was used only initially to assist in the desorption of water from the stainless steel tubing and was replaced by hydrogen as soon as the gas system was dry enough to start performing equilibrium experiments. The large difference in the equilibration period is presumably due to the large difference in gas viscosity values existing between the gases. The gas viscosity values relate to the molar mass of the gases and gases with large viscosity values exhibit lower diffusion rates. The equilibration period also depends on the size of Drierite particles (larger particles impose less restriction on gas diffusion) as well as the diffusion distance. Clearly, care has to be taken to determine the equilibration period for each individual case, if more than one type of Drierite column is used.

As indicated earlier, after a few days of monitoring the water content in the Argon gas stream, the water levels were sufficiently low to proceed with the experimental work. For this, glass reactors were used to contact the hydrogen with sulphuric acid solutions.

The already immersed reactors in the water bath are shown in figure 28.

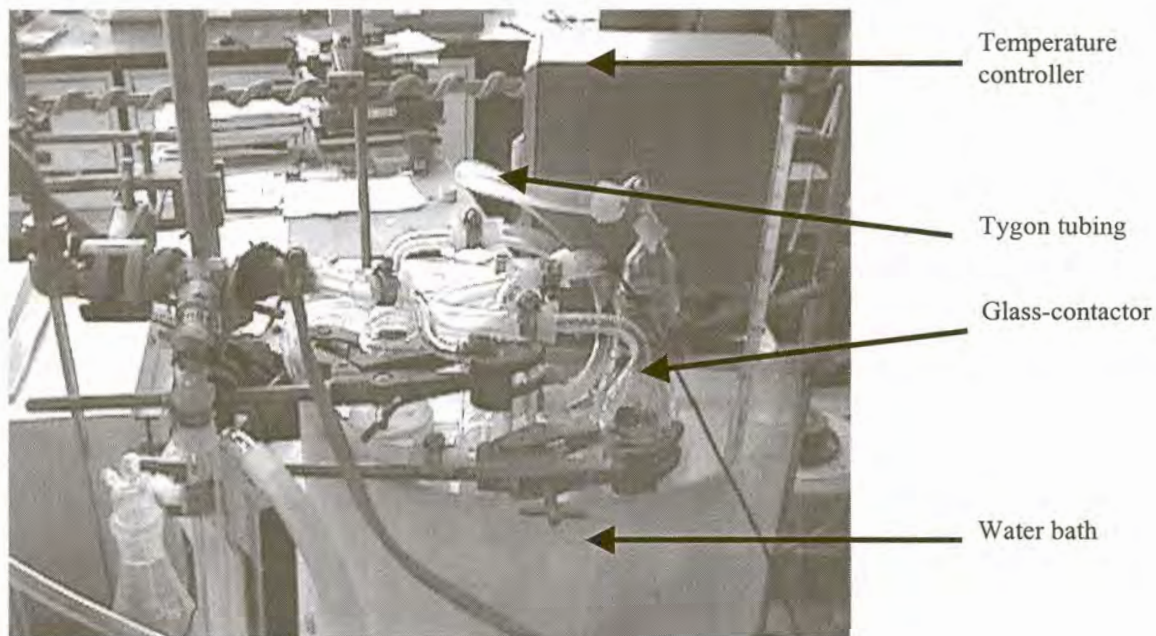


Figure 28: Photograph showing immersed glass reactors with temperature controller.

The inlets and outlets of two reactors were connected in series using flexible Tygon tubing. Hose clamps were used to ensure gas tightness of the connections. A pressure

drop of 11cm Hg over the reactors was observed. Although a dense polymer, the Tygon could not prevent gas from diffusing out resulting in a pressure drop within the gas line when not in use, causing the withdrawal of sulphuric acid from the reactors into the tubing. Attack of the tubing was prevented by keeping the reactors pressurised between experimental runs.

Each reactor contained about 0.5 dm<sup>3</sup> of sulphuric acid solution. The amount of water vapour in the gas stream was originally fixed by contacting the hydrogen gas with 85% sulphuric acid at a controlled temperature of  $60 \pm 0.1^\circ\text{C}$ . The first equilibrium run served the purpose to test the assumption that the activity of Al in FeV is similar to that of Al in dilute steel. This assumption was originally made in order to perform calculations to estimate the oxygen potential in the industrial smelting process. Results obtained will be discussed in more detail later in this work. (See section). Before this experiment could be performed, checks had to be performed on the exist gas composition to determine the consistency as well as the deviation from equilibrium, as been depicted by figure 29.

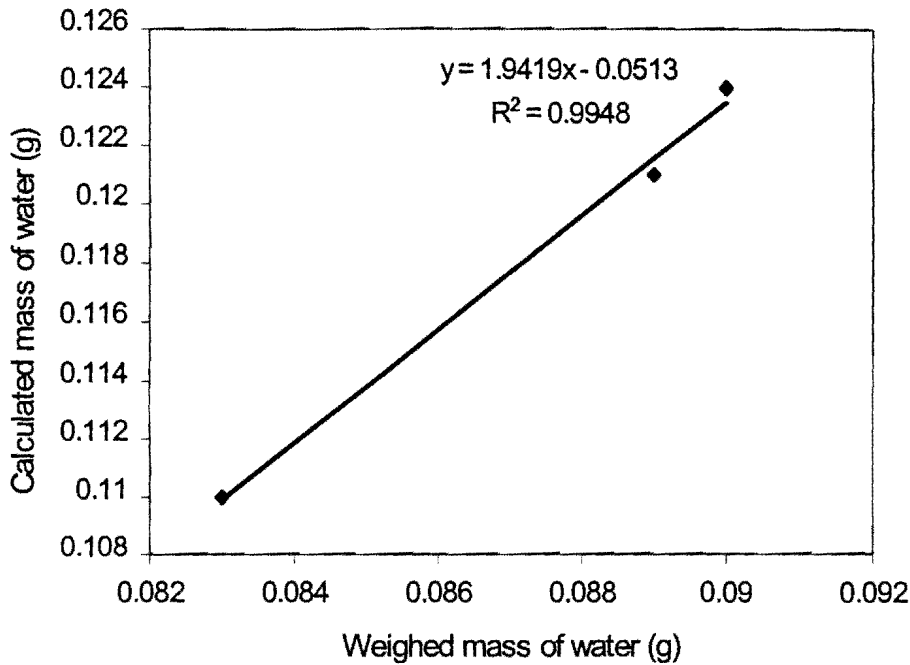


Figure 29: Comparison between the actual mass of water transported by the gas stream and the mass of water calculated assuming equilibrium between the water vapour in gas stream and acid. Calculations were performed for a 85 % sulphuric acid solution kept at 60°C. Gas flow rate of 0.18 NI/min and total pressure 0.877 atm were used. Tabulated correlations in Perry et al (1984) of the partial water pressure as a function of temperature and acid composition were also implemented. Values are for different times of gas flow, ranging from 19 to 24 hours.

Figure 29 shows that the amount of water in the reaction gas deviates considerably from the equilibrium calculated amount, thus indicating that the equilibrium could not be obtained within the saturators. In any case, equilibration of the lime-alumina slag with a vanadium crucible under this atmosphere caused a low vanadium oxide contact (of only 1%) compared with the 3% in plant slag. Because of too reducing condition the 85% sulphuric acid solution was replaced by a 75 % sulphuric acid solution at a controlled temperature of  $42 \pm 0.1^\circ\text{C}$ . The equilibrium partial water pressure above the surface of the sulfuric acid was thus increased by 2.7 times. The composition of the sulphuric acid solution was monitored prior to filling of the columns, by measuring of the density of sulphuric acid solutions. The density measurements were performed by immersing a piece of 316 stainless steel plate, the volume of which was accurately pre-determined ( $33.72\text{cm}^3$ ), into the sulphuric acid solution at a known temperature. After immersion, the

flat plate was weighed accurately to three decimal places, to measure the decrease in weight due to the buoyancy force acting on the flat plate. On average, the mass readings showed around 10 mg decrease due to the corrosion of the stainless steel in the sulphuric acid solution from the moment the reading stabilised until the reading was recorded. The density of the sulphuric acid can be calculated using the equation 45

$$\rho_{\text{H}_2\text{SO}_4} = \frac{\text{Weight of flat plate before immersion} - \text{Weight of flat plate after immersion}}{\text{Volume of flat plate}}$$

With  $\rho_{\text{H}_2\text{SO}_4}$  : density of sulphuric acid ( $\text{g}/\text{cm}^3$ )

(42)

A variation of  $0.010\text{g}/33.72 \text{ cm}^3$  yields an uncertainty of  $\pm 0.03\%$  in the density of the sulphuric acid.

Accurate tabulation of sulphuric acid densities as a function of temperature and composition is found in literature (Perry (1984)).

To ensure that conditions proceed as close as possible to equilibrium between the water vapour in the gas stream and acid, three glass reactors containing a helical gas-liquid contractor were employed in series. One such reactor is depicted in figure 30.

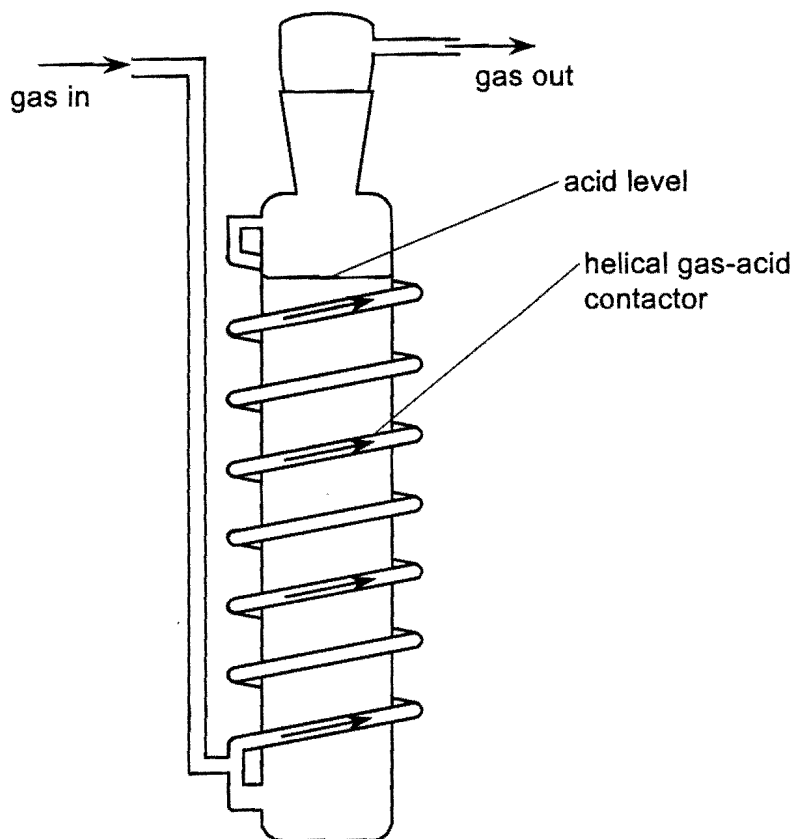


Figure 30: Glass contactor containing sulphuric acid, showing the path of the carrier gas.

The stainless steel tubing was protected from possible acid attack by using glass traps at the inlet and outlet of the sulphuric acid contractors as depicted in figure 31. The glass reactor preceding the water bath was dried at 200°C to ensure no gas stream contamination during its exposure to the atmosphere when the sulphuric acid was replaced. Concentrated sulphuric acid attacks 316 stainless steel tubing and precautionary measures had to be taken against sharp pressure fluctuations which may cause acid reaching the tubing.

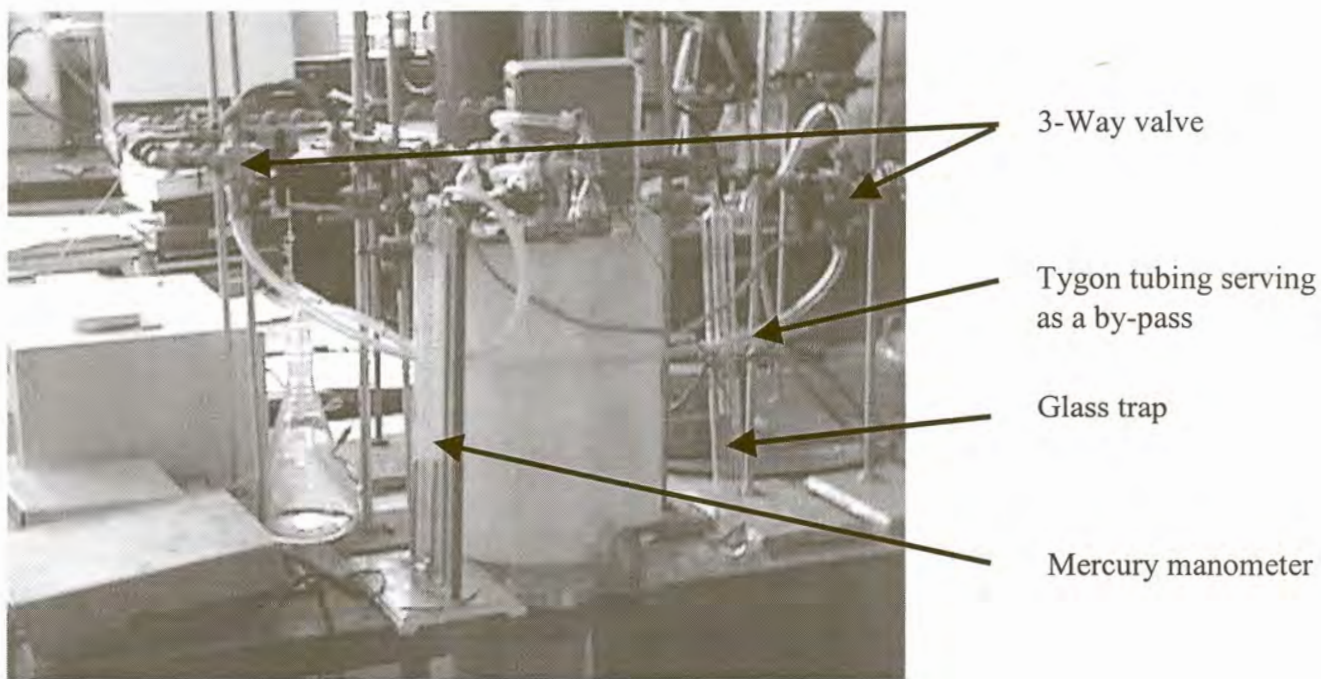


Figure 31: Glass traps used to protect 316 stainless steel tubing against acid spurts.

All three the reactors were immersed in a 25-liter plastic water bath ensuring good insulation against heat transfer to the environment. Atmospheric water pick-up, between experimental runs and during the replacement of the sulphuric acid reactors, was eliminated by using valves at the exposed open-ends of the stainless tubing, as depicted in figure 24. Three-way valves located on either side of the sulphuric acid reactors made it possible to by-pass the reactors when flushing with Argon gas was required. Unnecessary stripping of water out of sulphuric acid solutions was therefore avoided. The temperature of the water bath was accurately controlled to within  $0.1^{\circ}\text{C}$  using a Grant VFP thermostatic circulator. Calibrated thermometers were used additionally to monitor the water bath temperature in case the immersion thermostat failed to measure the temperature accurately. Recordings of the bath temperature were also continuously made for future reference.

The gas system contained two separate gas lines for Ar/He and  $\text{H}_2$ , which joined just before the rotameter. Oxygen was removed from the Argon or Helium by passing it over copper turnings held at  $600^{\circ}\text{C}$ . The copper-turning furnace was directly followed by an

anhydrous  $\text{CaSO}_4$ -filled column to remove any water. A second anhydrous  $\text{CaSO}_4$ -filled column was inserted just after the rotameter to remove any excess water entering the system through the hydrogen. At the outlet from the furnace, the hydrogen gas was burnt on a heated platinum wire after passing through an oil trap. Figure 32 shows the heated Pt-wire assembly.

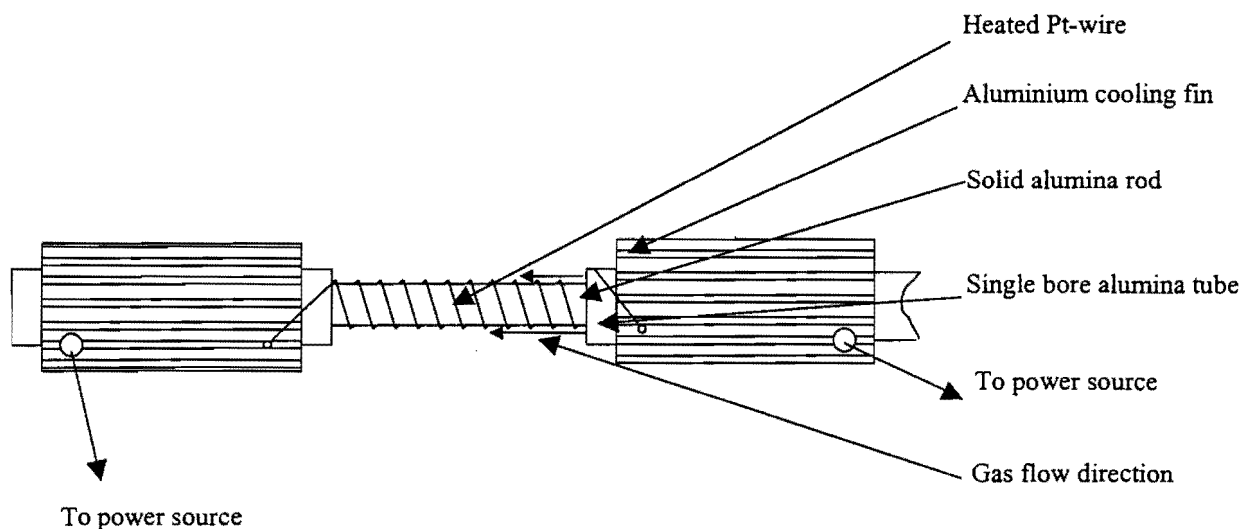


Figure 32: Heated platinum wire assembly.

The platinum wire assembly proved to be a safe alternative to the traditional bunsen-flame method of oxidation of hydrogen gas. The platinum wire was kept at around  $1000\text{ }^{\circ}\text{C}$  for weeks on end without failure. This enables experiments to be safely carried out throughout the night if no power failure occurs. The completeness of the oxidation reaction was determined by holding a hydrogen detector in the close vicinity of the heated platinum wire. No traces of excess hydrogen could be detected around the platinum wire. As can be indicated by the figure, the Pt-wire was wound around an alumina tube that fitted snugly into a larger alumina tube which directed the hydrogen gas through the small opening between the two tubes onto the hot Pt-wire. This ensured intimate contact between the hydrogen gas and the Pt-wire.

Gas flow rates were measured and controlled by a single rotameter which was calibrated in-line using a bubble meter. In-line calibration of the rotameter was required to establish the exact flow rate of the gas mixture because a back pressure in the gas line does affect

the flow rate. For this calibration purpose, the outlet from the oil trap at the end of the gas system was connected to the bottom of bubble meter cylinder. The gas was introduced into the bottom of the apparatus, displacing a soap bubble along the length to the top end of the cylinder. A stopwatch was used to establish the time required for one bubble to traverse the indicated volume. This measurement was repeated around 20 times to establish a good average value for each rotameter setting.

During actual equilibration runs, the hydrogen flow rate was kept at  $0.18 \text{ Ndm}^3/\text{min}$  throughout. Because equilibrium between the water vapour in the gas and acid can not be assumed, the actual amount of water in the gas was monitored (between equilibration runs) by passing the humid gas stream through a Drierite-filled column for a period of 5 hours. The mass increase was weighed accurately to the nearest milligram. The 5 hour exposure period yielded a typical mass increase of 85 mg. Figure 33 depicts the actual mass of water transferred per unit time, as a function of the total time that the sulphuric acid reactors were in use

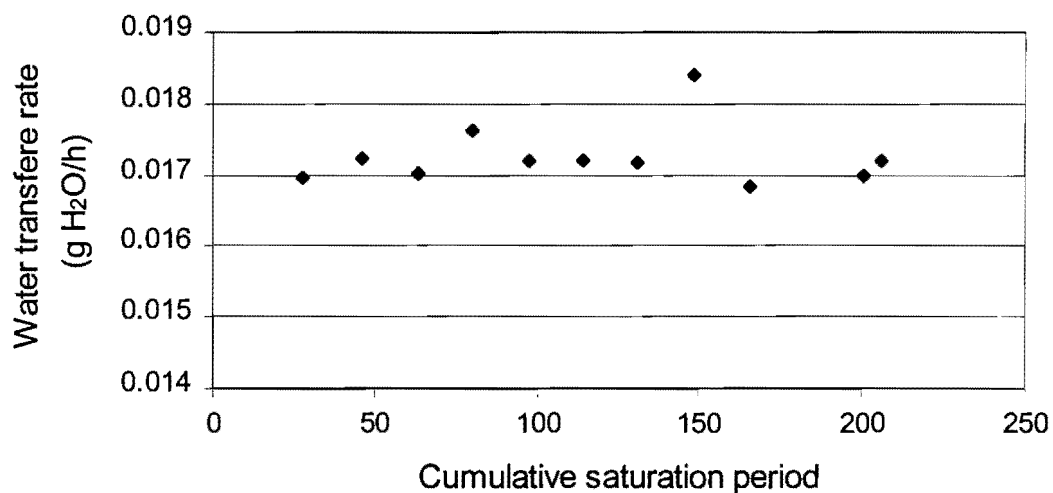


Figure 33: The actual mass of water measured per unit time as a function of the time the sulphuric acid reactors were in use.

As indicated by figure 33, no appreciable change in the water content of the reaction gas due to stripping of water out of the sulphuric acid occurred during the 200 hour saturation period.

The reliability of the measured mole fraction of water vapour depends on the accuracy of the weight measurements. A three-digit scale is in effect only accurate to two decimal places. The weighing practice was kept as consistent as possible to increase the reliability of the measurements. The resulting average calculated mole fraction of water vapour in the gas stream was  $(2.00 \pm 0.05) \times 10^{-3}$  for the equilibrium runs. In one experiment the mole fraction water vapour in the hydrogen gas was increased to  $(3.52 \pm 0.02) \times 10^{-3}$  to determine the oxidation state of vanadium in the slag.

Leak detection was performed before each equilibrium run by filling the gas line with pressurised Helium gas ( pressures around 12 cm Hg were applied) and checking for leaks with a hand-held helium detector. Leak checks performed on the furnace itself will be discussed later this section.

The line pressure before and after the water bath was measured using mercury manometers. The pressure above the acid solution is important for calculating the actual as well as equilibrium amount of water (mole fraction) in the hydrogen stream. Figure 34 compares the actual amount of water transferred, with the equilibrium amount of water (calculated using the following values and equation 25 in the literature section).

Acid composition: 75.7% H<sub>2</sub>SO<sub>4</sub> (determined from density measurements)

Water bath temperature: See appendix 1

Exposure period to acid reactors: See appendix 1

Gas flow rate: 0.18 NL/min

Total pressure above acid solution: 0.877 atmosphere

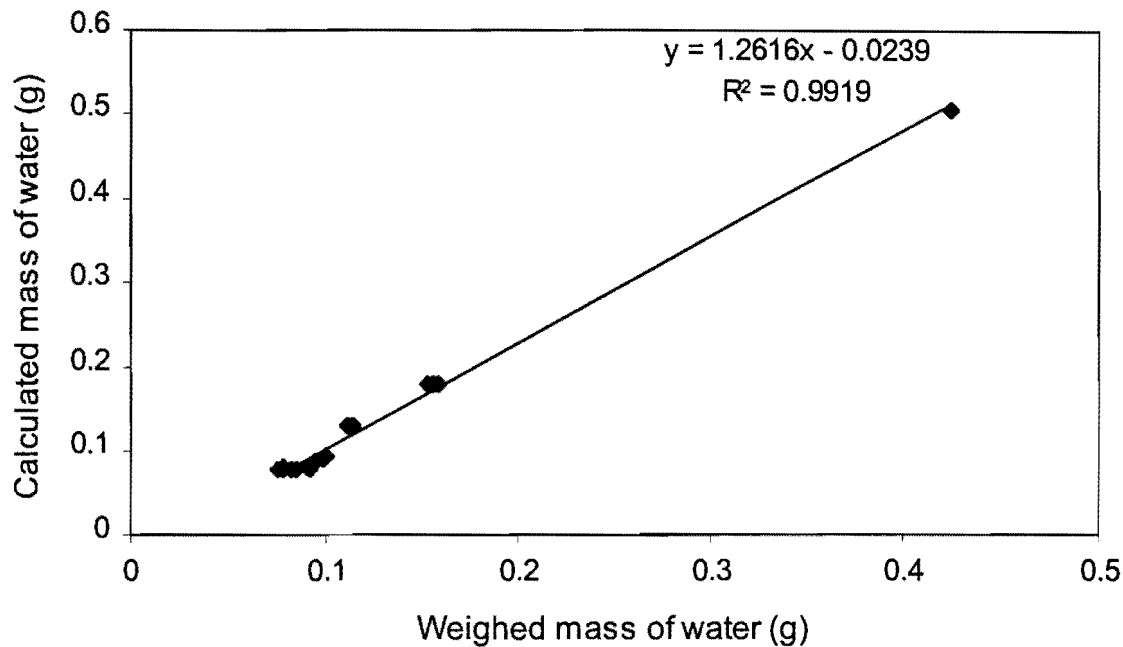


Figure 34: Comparison between the actual weighed mass of water and mass of water calculated assuming equilibrium between water vapour in the gas stream and the acid.

As figure 34 shows, checks performed on the exit gas composition using Drierite-filled columns show a definite deviation from the calculated water content of the reaction gas (calculated assuming equilibrium between the water vapour in the reaction gas and the sulphuric acid solution.) The amount of water in the reaction gas is consistently lower than the predicted content indicating that three reactors in series are not capable of obtaining the equilibrium water content in the reaction gas.

The slopes of the straight lines fitted through the data points in figure 29 and 34, indicate that the system utilising a 75 % sulphuric acid solution is closer to equilibrium than the system utilising a 85% sulphuric acid solution. It is thus easier to obtain equilibrium between the water vapour in the gas stream and the acid if the lower concentration sulphuric acid solution is utilised.

The reactors were designed at first with helical contactors, measuring a total length of around 6 meters, to ensure long intimate contact between the reaction gas and sulphuric acid solution. Despite obvious measures to ensure equilibrium, at the end equilibrium

could not be obtained. This underlines the fact that checks on the exit gas composition between equilibrium runs are absolutely essential. Any published data based on  $H_2/H_2O$ -equilibrium utilised to fix the oxygen activity should contain the method used to determine the gas composition. An assumption that equilibrium conditions prevail in the saturator may decrease the value of the work. It can further be concluded that the water content of the reaction gas can be successfully monitored using Drierite as absorbent.

The sulphuric acid solution (after more than 200 hours exposure period) was replaced after the completion of the first series of experiments investigating activity-composition relations. Table 15 shows the calculated composition of the sulphuric acid in the reactors before and after the completion of the experiments

	Initial Composition	Final composition
First reactor	75.7	75.5
Second reactor	75.7	75.2
Last reactor	75.7	75.2

Table 15: Change in sulphuric acid composition. (mass percentages)

It is evident that no appreciable change of the sulphuric acid composition occurred and that 200 hours' exposure with 3 reactors containing  $0.5 \text{ dm}^3$  acid can comfortably maintain a constant water vapour level in the hydrogen gas.

### **2.2.2. The furnace set-up**

A schematic representation of the furnace assembly set-up is shown in figure 35.

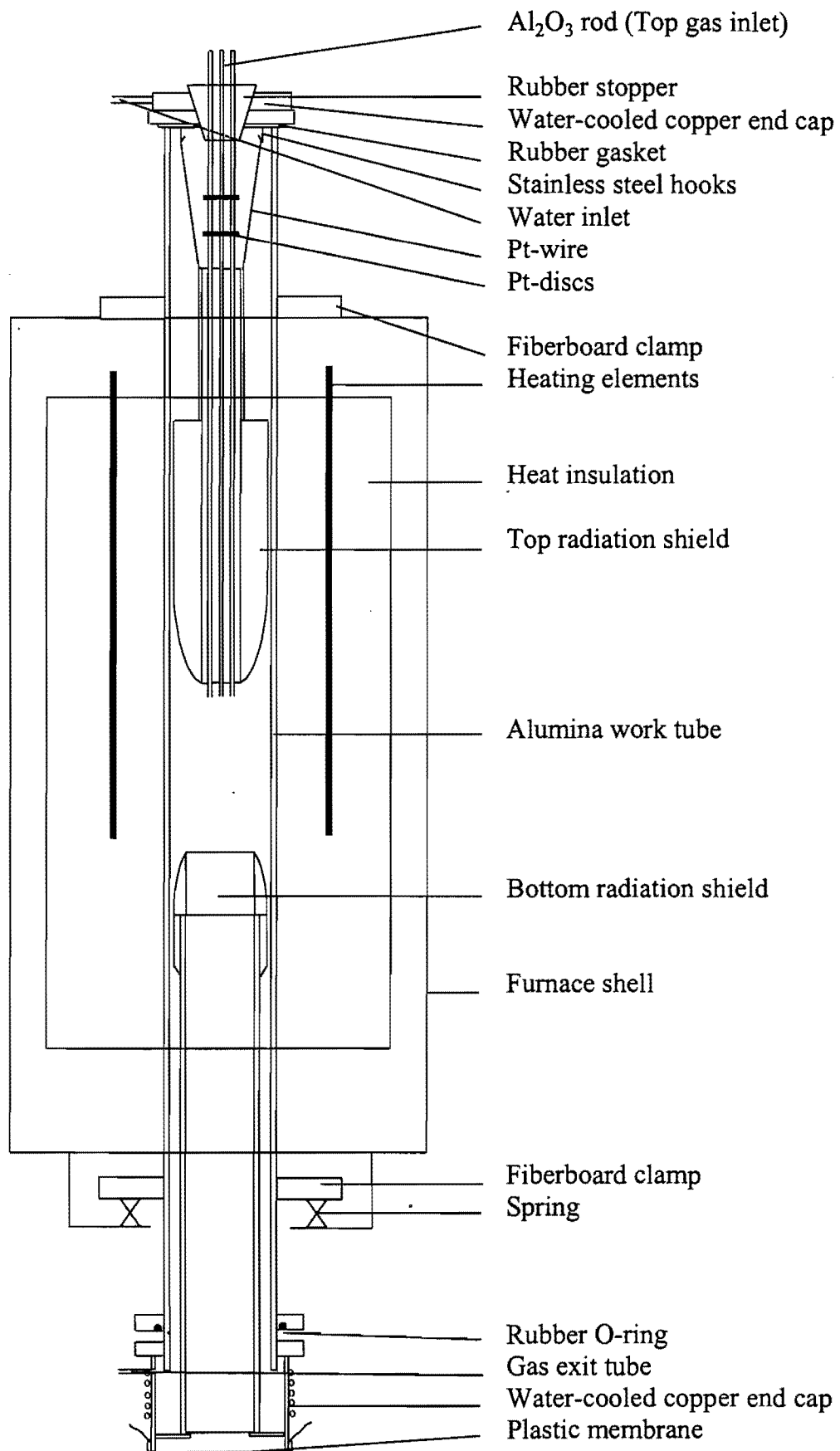


Figure 35: Schematic representation of the furnace assembly set-up

The vertical tube resistance furnace from Pirotherm which employed six equidistant molybdenum disilicide-tungsten carbide heating elements, situated around the furnace tube, was utilized. The specified temperature rating of the furnace is maximum 1800°C for normal heating and cooling cycle. If necessary the furnace could reach 1850°C whereafter the elements should never be switched off and kept at or above 900°C indefinitely.

The maximum temperature that could reliably be obtained in the available laboratory furnace without drastically reducing the life of the elements, was 1700°C. To test the temperature influence on the activity coefficient of vanadium, an experiment was conducted at 1750°C. Due to severe SiO<sub>2</sub> pick-up in the slag no more experiments were performed at this temperature. A single run at 1650 °C was performed to test the influence of temperature on the activity coefficient of vanadium.

The furnace temperature was controlled by an Eurotherm controller/programmer using a Pt-40%Rh/Pt-20%Rh thermocouple that was positioned next to the furnace tube, close to the hot zone. The exact position and temperature of the hot zone was measured with a hand-held Pt-40%Rh/Pt-20%Rh thermocouple (Bedford,1965) placed at various depths in the furnace tube. During this procedure the lower end of the alumina tube was covered with a plastic film to prevent an updraft of hot air through the furnace tube leading to inaccurate measurements. The temperature profile as a function of position at a programmed temperature of 1600°C is shown in figure 36.

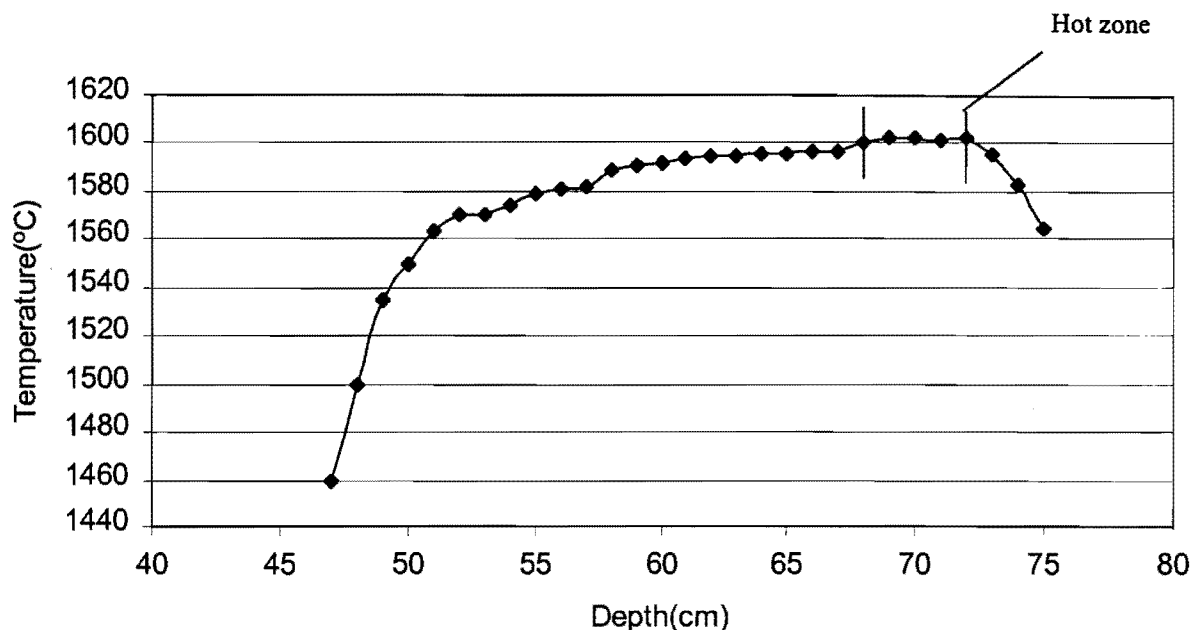


Figure 36: Temperature profile as a function of position. Depth measured from top of alumina tube. Programmed furnace temperature:1600°C; the furnace hot zone was determined to be 50 mm in length. The average measured temperature in this zone was (1601±0.5 °C).

The average temperature of the hot zone measured with the hand-held thermocouple was within 1°C of that indicated by the furnace controller.

The re-crystallized alumina (99.8% Al<sub>2</sub>O<sub>3</sub>) furnace tube (length 1.2m, O.D. 75 mm, and I.D. 65 mm) was fitted with water-cooled copper heads at both ends. The bottom fitting extended below the alumina tube and was sealed with O-rings lubricated with high temperature vacuum grease. The upper end cap was sealed, before each equilibrium run, to the open flat end of the tube, sealing with a rubber gasket between the tube and the fitting. A steel bracket attached to the furnace tube exerted pressure on the gasket. The upper end cap contained the rubber plug sealed to the fitting, to prevent gas leakage due to the high pressure within the work tube. The rubber plug was used as exit seal for the three alumina tubes used to suspend the vanadium crucible inside the tube and to introduce gas to the synthetic slag. The tubes were sealed to the rubber plug with silicone sealer.

Possible thermal damage (by radiation from the hot zone) to the rubber plug and silicone sealant was prevented by using two round Pt discs fixed to the alumina tubes using Pt-wire. The Pt-disc diameters corresponded to the inside diameter of the alumina tube, which formed part of the upper radiation shield. No thermal damage whatsoever was observed at the surface of the rubber plug.

Radiation shields were present within the furnace tube above and below the crucible. The purpose of top radiation shield was to protect the elements as well as copper end cap from excessive temperatures. The top radiation shield was suspended from the water cooled end cap using 0.5 mm O.D. Pt-wire.

Failure of the vanadium crucible during the first equilibrium run due to complete melting was found to be the result of severe phosphorus pick-up. The radiation shields consisted of fibreboard rings made from a high-temperature fibreboard, temperature rating of 1800°C, and glued together using high temperature cement. The cement originally used to manufacture the radiation shield was an alumina-phosphate cement. Under reducing high-temperature conditions, the cement can be reduced to  $\text{Al}_2\text{O}_3$  and  $\text{P}_2$  (gas). The phosphorus gas apparently alloyed with the vanadium crucible to form a low melting point eutectic component resulting in failure at a temperature 200°C below the melting point of pure vanadium. The radiation shields were reconstructed using the same high-temperature fibreboard rings and pure high-temperature alumina cement. Following severe silica pick-up in the slag within the crucible during early runs, these radiation shields were found to contain mullite, which can be reduced to  $\text{Al}_2\text{O}_3$  and  $\text{SiO}(\text{g})$  under reducing high-temperature conditions employed here. In support of this mechanism, silica crystals were observed on the cooler regions of the radiation shields. The continuous precipitation of silica onto the gas carrying alumina tube over extended periods led to failure of the tube due to glass formation. A glass phase could clearly be observed in the vicinity of the crack formed in the alumina tube.

The radiation shields were originally coated with a  $\pm 5$  mm thick layer of alumina (98%  $\text{Al}_2\text{O}_3$ ), applied as a slurry. The alumina layer was subsequently sintered at 1400°C for at least 8 hours in a muffle furnace. The alumina coating and sintering cycle were repeated a number of times, if considered necessary, after the radiation shield was examined for

large cracks. Some cracking of the alumina coating did still occur during subsequent use, causing sporadic contamination of the samples by silica. Those samples which showed more than 2 % silica (mass percentage) pick-up were discarded. Silica pick-up was more severe in slags with higher basicities, presumably due to low silica activity coefficients in these slags. Furthermore, there was a direct correlation between the creep behaviour and the silica content of the slags. Severe slag creep was observed in some early experiments due to severe silica pick-up from radiation shields. Slag creep was prevented, to an extent, by reducing silica pick-up by coating the radiation shields, machining two grooves into the inner wall near the top of crucible and also by dividing the opening of the crucible into two using a 0.1mm vanadium wire (See figure 38).

### **2.2.3. Quenching set-up.**

The lower-end of the furnace tube was sealed with a PVC membrane, thickness of 30  $\mu\text{m}$ , wrapped over the furnace tube opening, with a layer of vacuum grease as sealant between the copper end cap tube and the plastic film. The PVC film was held in position by using a hose clamp pressing onto a (0.1 mm-thick, 20mm wide) PVC band preventing the thin plastic film from being cut by the clamp.

The PVC-covered end cap was immersed in water, contained in an aluminium container through which water ran continuously. A large container/reservoir situated below the aluminium container was continuously filled by the overflow of the top container. When the water level within the reservoir reached a certain height, a pressure sensitive switch activated a pump located at the bottom of the reservoir.

The quenching set-up shown in figure 37, consisted of two single bore alumina tubes (I.D. 2.5 mm) containing molybdenum wires of 1 mm in diameter. The bottom protruding molybdenum wires were bent to form two hooks. The top hole from which the thick wires protruded (above the furnace tube) was sealed by silicone sealant. The crucible was suspended from the two molybdenum wire hooks by means of a thinner (0.3 mm diameter) connecting molybdenum wire. Solid-state diffusion is very much possible at 1700 °C and ultra-low partial oxygen pressures result in oxide-free contact surfaces. Solid-state welding occurred between the thick molybdenum hooks and the thin

anhydrous  $\text{CaSO}_4$ -filled column to remove any water. A second anhydrous  $\text{CaSO}_4$ -filled column was inserted just after the rotameter to remove any excess water entering the system through the hydrogen. At the outlet from the furnace, the hydrogen gas was burnt on a heated platinum wire after passing through an oil trap. Figure 32 shows the heated Pt-wire assembly.

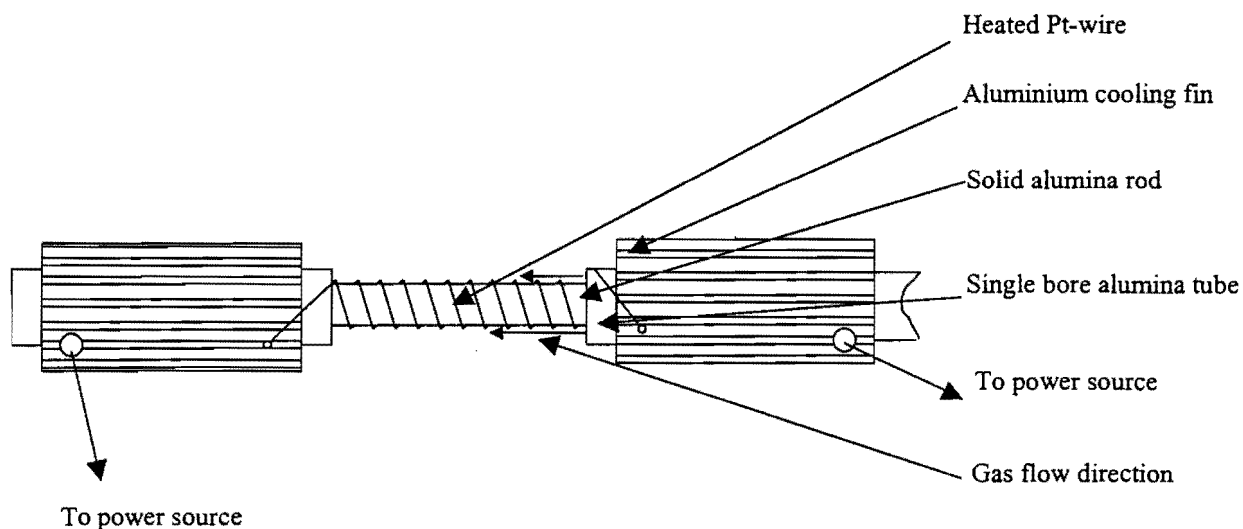


Figure 32: Heated platinum wire assembly.

The platinum wire assembly proved to be a safe alternative to the traditional bunsen-flame method of oxidation of hydrogen gas. The platinum wire was kept at around  $1000\text{ }^{\circ}\text{C}$  for weeks on end without failure. This enables experiments to be safely carried out throughout the night if no power failure occurs. The completeness of the oxidation reaction was determined by holding a hydrogen detector in the close vicinity of the heated platinum wire. No traces of excess hydrogen could be detected around the platinum wire. As can be indicated by the figure, the Pt-wire was wound around an alumina tube that fitted snugly into a larger alumina tube which directed the hydrogen gas through the small opening between the two tubes onto the hot Pt-wire. This ensured intimate contact between the hydrogen gas and the Pt-wire.

Gas flow rates were measured and controlled by a single rotameter which was calibrated in-line using a bubble meter. In-line calibration of the rotameter was required to establish the exact flow rate of the gas mixture because a back pressure in the gas line does affect

the flow rate. For this calibration purpose, the outlet from the oil trap at the end of the gas system was connected to the bottom of bubble meter cylinder. The gas was introduced into the bottom of the apparatus, displacing a soap bubble along the length to the top end of the cylinder. A stopwatch was used to establish the time required for one bubble to traverse the indicated volume. This measurement was repeated around 20 times to establish a good average value for each rotameter setting.

During actual equilibration runs, the hydrogen flow rate was kept at  $0.18 \text{ Ndm}^3/\text{min}$  throughout. Because equilibrium between the water vapour in the gas and acid can not be assumed, the actual amount of water in the gas was monitored (between equilibration runs) by passing the humid gas stream through a Drierite-filled column for a period of 5 hours. The mass increase was weighed accurately to the nearest milligram. The 5 hour exposure period yielded a typical mass increase of 85 mg. Figure 33 depicts the actual mass of water transferred per unit time, as a function of the total time that the sulphuric acid reactors were in use

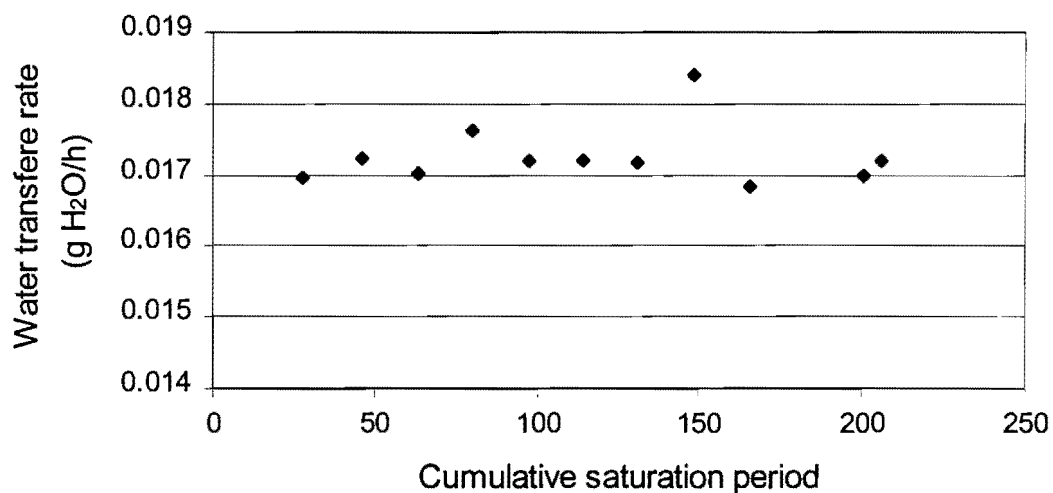


Figure 33: The actual mass of water measured per unit time as a function of the time the sulphuric acid reactors were in use.

As indicated by figure 33, no appreciable change in the water content of the reaction gas due to stripping of water out of the sulphuric acid occurred during the 200 hour saturation period.

The reliability of the measured mole fraction of water vapour depends on the accuracy of the weight measurements. A three-digit scale is in effect only accurate to two decimal places. The weighing practice was kept as consistent as possible to increase the reliability of the measurements. The resulting average calculated mole fraction of water vapour in the gas stream was  $(2.00 \pm 0.05) \times 10^{-3}$  for the equilibrium runs. In one experiment the mole fraction water vapour in the hydrogen gas was increased to  $(3.52 \pm 0.02) \times 10^{-3}$  to determine the oxidation state of vanadium in the slag.

Leak detection was performed before each equilibrium run by filling the gas line with pressurised Helium gas ( pressures around 12 cm Hg were applied) and checking for leaks with a hand-held helium detector. Leak checks performed on the furnace itself will be discussed later this section.

The line pressure before and after the water bath was measured using mercury manometers. The pressure above the acid solution is important for calculating the actual as well as equilibrium amount of water (mole fraction) in the hydrogen stream. Figure 34 compares the actual amount of water transferred, with the equilibrium amount of water (calculated using the following values and equation 25 in the literature section).

Acid composition: 75.7% H<sub>2</sub>SO<sub>4</sub> (determined from density measurements)

Water bath temperature: See appendix 1

Exposure period to acid reactors: See appendix 1

Gas flow rate: 0.18 NL/min

Total pressure above acid solution: 0.877 atmosphere

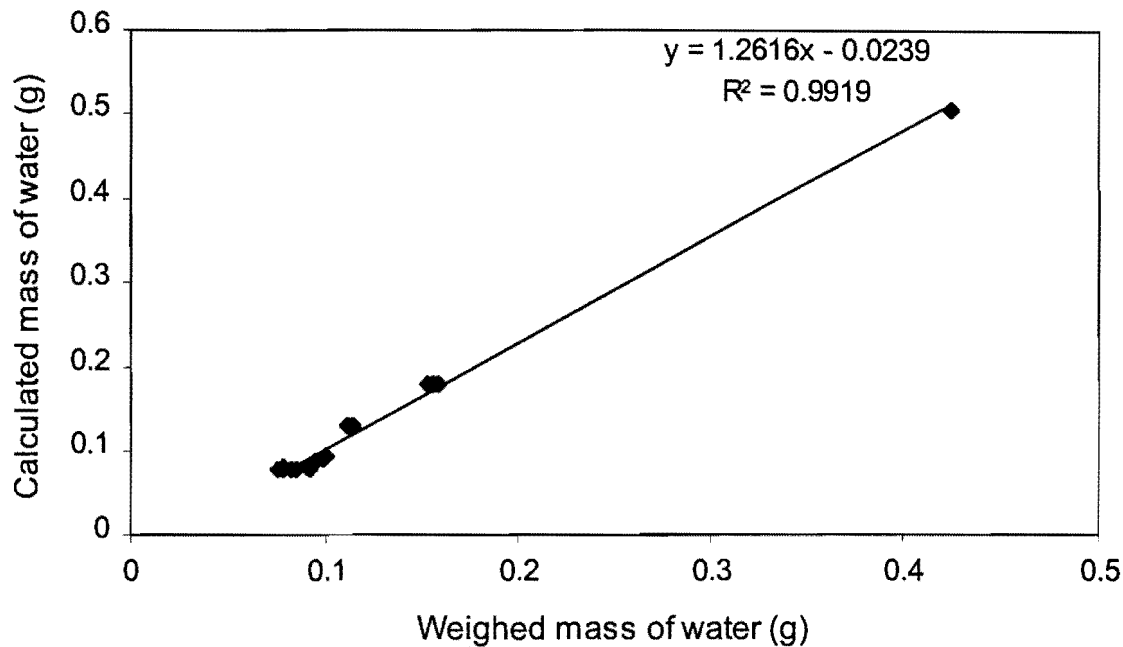


Figure 34: Comparison between the actual weighed mass of water and mass of water calculated assuming equilibrium between water vapour in the gas stream and the acid.

As figure 34 shows, checks performed on the exit gas composition using Drierite-filled columns show a definite deviation from the calculated water content of the reaction gas (calculated assuming equilibrium between the water vapour in the reaction gas and the sulphuric acid solution.) The amount of water in the reaction gas is consistently lower than the predicted content indicating that three reactors in series are not capable of obtaining the equilibrium water content in the reaction gas.

The slopes of the straight lines fitted through the data points in figure 29 and 34, indicate that the system utilising a 75 % sulphuric acid solution is closer to equilibrium than the system utilising a 85% sulphuric acid solution. It is thus easier to obtain equilibrium between the water vapour in the gas stream and the acid if the lower concentration sulphuric acid solution is utilised.

The reactors were designed at first with helical contactors, measuring a total length of around 6 meters, to ensure long intimate contact between the reaction gas and sulphuric acid solution. Despite obvious measures to ensure equilibrium, at the end equilibrium

could not be obtained. This underlines the fact that checks on the exit gas composition between equilibrium runs are absolutely essential. Any published data based on  $H_2/H_2O$ -equilibrium utilised to fix the oxygen activity should contain the method used to determine the gas composition. An assumption that equilibrium conditions prevail in the saturator may decrease the value of the work. It can further be concluded that the water content of the reaction gas can be successfully monitored using Drierite as absorbent.

The sulphuric acid solution (after more than 200 hours exposure period) was replaced after the completion of the first series of experiments investigating activity-composition relations. Table 15 shows the calculated composition of the sulphuric acid in the reactors before and after the completion of the experiments

	Initial Composition	Final composition
First reactor	75.7	75.5
Second reactor	75.7	75.2
Last reactor	75.7	75.2

Table 15: Change in sulphuric acid composition. (mass percentages)

It is evident that no appreciable change of the sulphuric acid composition occurred and that 200 hours' exposure with 3 reactors containing  $0.5 \text{ dm}^3$  acid can comfortably maintain a constant water vapour level in the hydrogen gas.

### **2.2.2. The furnace set-up**

A schematic representation of the furnace assembly set-up is shown in figure 35.

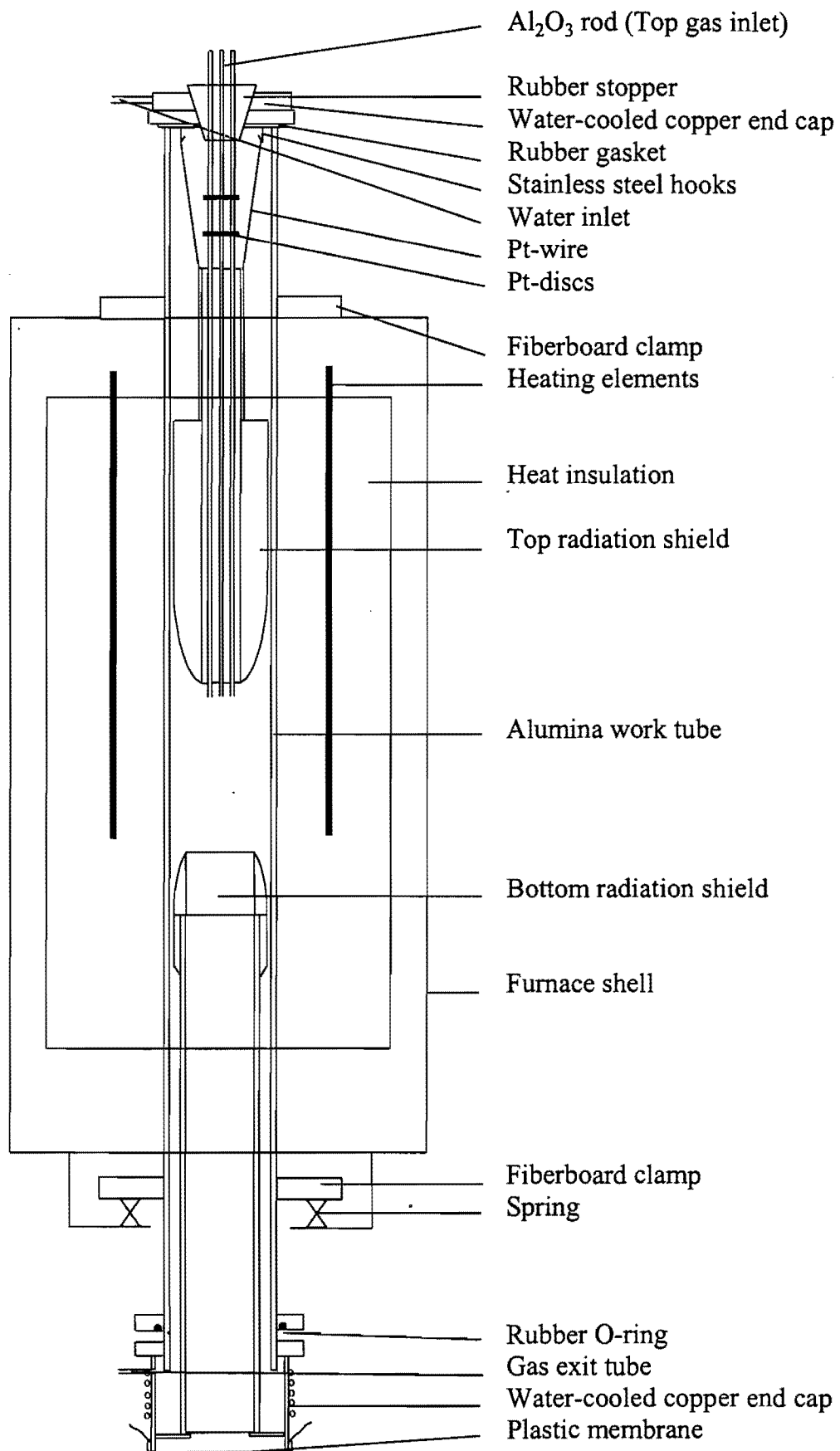


Figure 35: Schematic representation of the furnace assembly set-up

The vertical tube resistance furnace from Pirotherm which employed six equidistant molybdenum disilicide-tungsten carbide heating elements, situated around the furnace tube, was utilized. The specified temperature rating of the furnace is maximum 1800°C for normal heating and cooling cycle. If necessary the furnace could reach 1850°C whereafter the elements should never be switched off and kept at or above 900°C indefinitely.

The maximum temperature that could reliably be obtained in the available laboratory furnace without drastically reducing the life of the elements, was 1700°C. To test the temperature influence on the activity coefficient of vanadium, an experiment was conducted at 1750°C. Due to severe SiO<sub>2</sub> pick-up in the slag no more experiments were performed at this temperature. A single run at 1650 °C was performed to test the influence of temperature on the activity coefficient of vanadium.

The furnace temperature was controlled by an Eurotherm controller/programmer using a Pt-40%Rh/Pt-20%Rh thermocouple that was positioned next to the furnace tube, close to the hot zone. The exact position and temperature of the hot zone was measured with a hand-held Pt-40%Rh/Pt-20%Rh thermocouple (Bedford,1965) placed at various depths in the furnace tube. During this procedure the lower end of the alumina tube was covered with a plastic film to prevent an updraft of hot air through the furnace tube leading to inaccurate measurements. The temperature profile as a function of position at a programmed temperature of 1600°C is shown in figure 36.

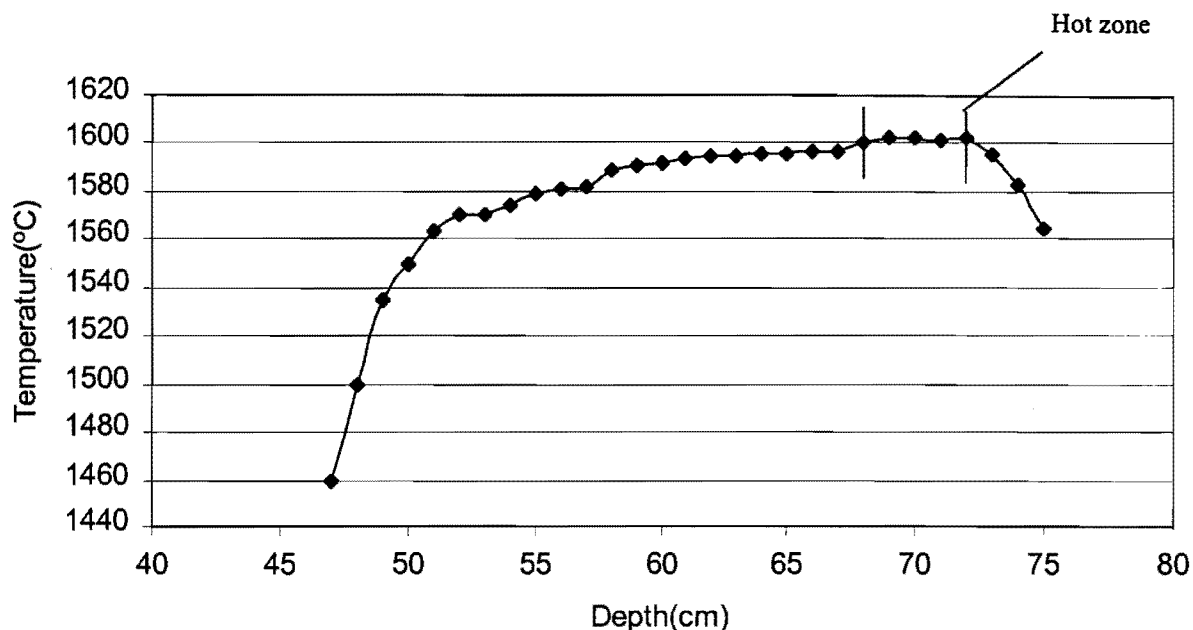


Figure 36: Temperature profile as a function of position. Depth measured from top of alumina tube. Programmed furnace temperature:1600°C; the furnace hot zone was determined to be 50 mm in length. The average measured temperature in this zone was (1601±0.5 °C).

The average temperature of the hot zone measured with the hand-held thermocouple was within 1°C of that indicated by the furnace controller.

The re-crystallized alumina (99.8% Al<sub>2</sub>O<sub>3</sub>) furnace tube (length 1.2m, O.D. 75 mm, and I.D. 65 mm) was fitted with water-cooled copper heads at both ends. The bottom fitting extended below the alumina tube and was sealed with O-rings lubricated with high temperature vacuum grease. The upper end cap was sealed, before each equilibrium run, to the open flat end of the tube, sealing with a rubber gasket between the tube and the fitting. A steel bracket attached to the furnace tube exerted pressure on the gasket. The upper end cap contained the rubber plug sealed to the fitting, to prevent gas leakage due to the high pressure within the work tube. The rubber plug was used as exit seal for the three alumina tubes used to suspend the vanadium crucible inside the tube and to introduce gas to the synthetic slag. The tubes were sealed to the rubber plug with silicone sealer.

Possible thermal damage (by radiation from the hot zone) to the rubber plug and silicone sealant was prevented by using two round Pt discs fixed to the alumina tubes using Pt-wire. The Pt-disc diameters corresponded to the inside diameter of the alumina tube, which formed part of the upper radiation shield. No thermal damage whatsoever was observed at the surface of the rubber plug.

Radiation shields were present within the furnace tube above and below the crucible. The purpose of top radiation shield was to protect the elements as well as copper end cap from excessive temperatures. The top radiation shield was suspended from the water cooled end cap using 0.5 mm O.D. Pt-wire.

Failure of the vanadium crucible during the first equilibrium run due to complete melting was found to be the result of severe phosphorus pick-up. The radiation shields consisted of fibreboard rings made from a high-temperature fibreboard, temperature rating of 1800°C, and glued together using high temperature cement. The cement originally used to manufacture the radiation shield was an alumina-phosphate cement. Under reducing high-temperature conditions, the cement can be reduced to  $\text{Al}_2\text{O}_3$  and  $\text{P}_2$  (gas). The phosphorus gas apparently alloyed with the vanadium crucible to form a low melting point eutectic component resulting in failure at a temperature 200°C below the melting point of pure vanadium. The radiation shields were reconstructed using the same high-temperature fibreboard rings and pure high-temperature alumina cement. Following severe silica pick-up in the slag within the crucible during early runs, these radiation shields were found to contain mullite, which can be reduced to  $\text{Al}_2\text{O}_3$  and  $\text{SiO}(\text{g})$  under reducing high-temperature conditions employed here. In support of this mechanism, silica crystals were observed on the cooler regions of the radiation shields. The continuous precipitation of silica onto the gas carrying alumina tube over extended periods led to failure of the tube due to glass formation. A glass phase could clearly be observed in the vicinity of the crack formed in the alumina tube.

The radiation shields were originally coated with a  $\pm 5$  mm thick layer of alumina (98%  $\text{Al}_2\text{O}_3$ ), applied as a slurry. The alumina layer was subsequently sintered at 1400°C for at least 8 hours in a muffle furnace. The alumina coating and sintering cycle were repeated a number of times, if considered necessary, after the radiation shield was examined for

large cracks. Some cracking of the alumina coating did still occur during subsequent use, causing sporadic contamination of the samples by silica. Those samples which showed more than 2 % silica (mass percentage) pick-up were discarded. Silica pick-up was more severe in slags with higher basicities, presumably due to low silica activity coefficients in these slags. Furthermore, there was a direct correlation between the creep behaviour and the silica content of the slags. Severe slag creep was observed in some early experiments due to severe silica pick-up from radiation shields. Slag creep was prevented, to an extent, by reducing silica pick-up by coating the radiation shields, machining two grooves into the inner wall near the top of crucible and also by dividing the opening of the crucible into two using a 0.1mm vanadium wire (See figure 38).

### **2.2.3. Quenching set-up.**

The lower-end of the furnace tube was sealed with a PVC membrane, thickness of 30  $\mu\text{m}$ , wrapped over the furnace tube opening, with a layer of vacuum grease as sealant between the copper end cap tube and the plastic film. The PVC film was held in position by using a hose clamp pressing onto a (0.1 mm-thick, 20mm wide) PVC band preventing the thin plastic film from being cut by the clamp.

The PVC-covered end cap was immersed in water, contained in an aluminium container through which water ran continuously. A large container/reservoir situated below the aluminium container was continuously filled by the overflow of the top container. When the water level within the reservoir reached a certain height, a pressure sensitive switch activated a pump located at the bottom of the reservoir.

The quenching set-up shown in figure 37, consisted of two single bore alumina tubes (I.D. 2.5 mm) containing molybdenum wires of 1 mm in diameter. The bottom protruding molybdenum wires were bent to form two hooks. The top hole from which the thick wires protruded (above the furnace tube) was sealed by silicone sealant. The crucible was suspended from the two molybdenum wire hooks by means of a thinner (0.3 mm diameter) connecting molybdenum wire. Solid-state diffusion is very much possible at 1700 °C and ultra-low partial oxygen pressures result in oxide-free contact surfaces. Solid-state welding occurred between the thick molybdenum hooks and the thin

connecting wire preventing quenching of the sample after equilibration when a current was passed through the molybdenum wires. This welding problem was prevented by applying graphite dag to the molybdenum wire hooks.

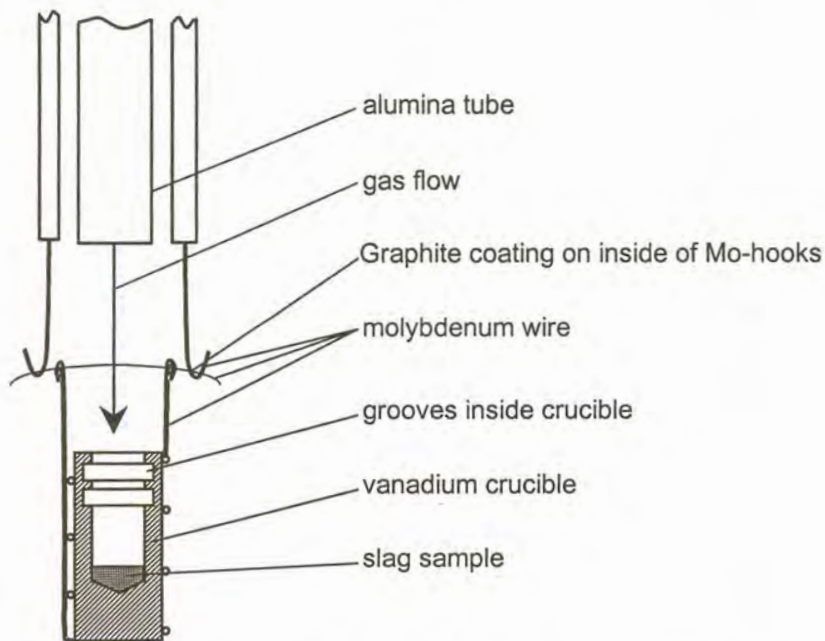


Figure 37: Detail of the configuration used to suspend the vanadium crucible inside the tube furnace, and to bring the reaction gas into contact with the slag.

Post-experimental investigations of the alumina tubes containing the thick Mo-wire showed a continuous layer of black dust, suggesting possible sublimation of the carbon at the experimental conditions. No visible carbon layer was observed on the Molybdenum hooks exposed to 1700°C, in contrast with the experiment performed at 1650°C where a small amount of carbon could be observed. A much larger applied potential was needed to melt the bridge wire in case of the 1650°C-experiment indicating the possible occurrence of a relative thick layer of carbon compared to the layer at 1700°C. Nevertheless, the carbon coating of the hooks has proven to be a successful measure against molybdenum welding under high-temperature reducing conditions.

The sample was hence removed from the furnace by applying an electrical current to the thick molybdenum wires protruding from the top of the alumina tube. This led to the melting of the thinner wire, subsequently releasing the crucible to fall through the PVC membrane into the container containing water. Rapid cooling of the quenched sample was hindered by a water vapour "blanket" surrounding the crucible. Despite expecting a

homogenous glass phase to be present in the vanadium crucible, some slags contained a number of non-equilibrium phases resulting in larger variations on the analysed mole fraction vanadium in the slag. (See the section 2.3.3. on sample analysis).

#### 2.2.4. Crucibles

Equilibration of the slag with the selected gas composition was performed in vanadium crucibles. The crucibles were manufactured by turning and drilling the crucibles out of high purity vanadium rod. (99,9%). The dimensions of the crucible are given in figure 38.

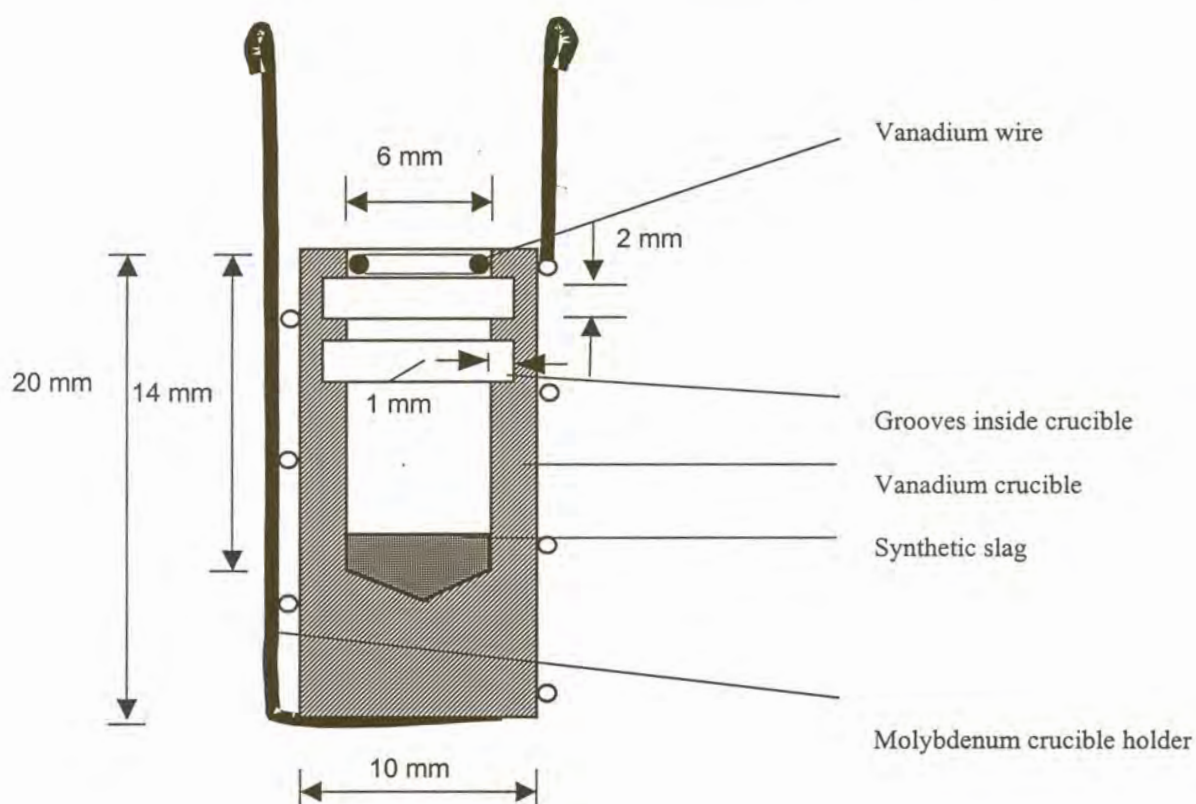


Figure 38: Schematic representation of pure vanadium crucible being used.

By using a pure vanadium crucible, the use of a separate metal phase was avoided. The vanadium crucible supplied all the vanadium needed to attain equilibrium between the container and vanadium oxide in the synthetic slag. Each crucible was contained in a wire crucible holder made from 1 mm diameter molybdenum wire. The crucible holder

## 2.3. Experimental procedure

### 2.3.1. Slag preparation

The maximum temperature that could be obtained reliably in the available laboratory furnace was 1700 °C. The CaO-Al<sub>2</sub>O<sub>3</sub> slag investigated in this study covered the range of liquid compositions at 1700°C as shown in figure 39 and Table 16.

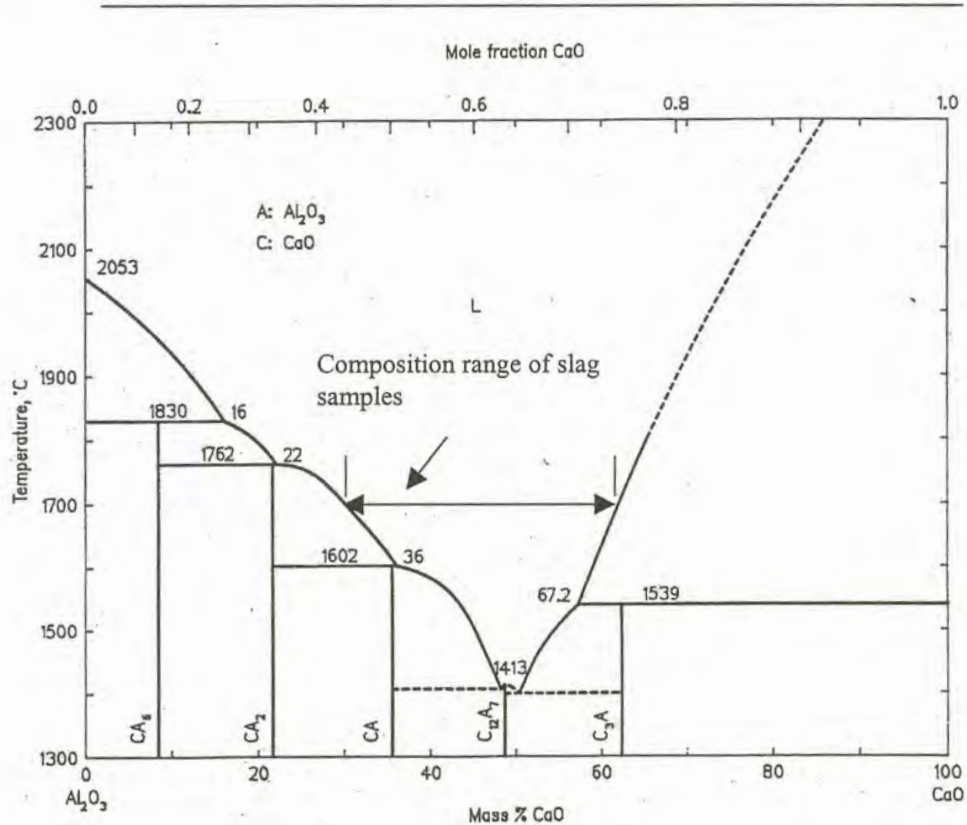


Figure 39: CaO-Al<sub>2</sub>O<sub>3</sub> phase diagram showing the composition range of the slag samples (Verein Deutscher Eisenhüttenleute,1995).

	Slag 1	Slag 2	Slag 3	Slag 4	Slag 5	Slag 6	Slag 7
% CaO	25	33	29	41	49	37	45
% Al <sub>2</sub> O <sub>3</sub>	75	67	71	59	51	63	55

Table 16 : As-mixed compositions (mass percent) of the slag melts studied.

The following chemicals were used to make up the slag mixtures shown in Table 15 before equilibration: GP-grade  $V_2O_5$  (assay: >99%), V (assay: 99.9%),  $CaCO_3$  (assay: 99.5%), MgO (assay: 98%) and  $Al_2O_3$  (assay: 99%). The first few experiments concentrated on the effect of MgO on the amount of oxidic vanadium in slag. Unfortunately, it was not possible to establish the effect of MgO under equilibrium conditions. No MgO originally added to the slag samples could be retained after equilibration because magnesium has a significant equilibrium vapour pressure. (See section in literature study). It was subsequently assumed that MgO behaves similarly to CaO in the industrial furnace on a molar basis (as far as the effect on  $VO_x$  activity is concerned) because both oxides show strong basic behavior in low basicity slags. For this reason, the experimental work concentrated on CaO- $Al_2O_3$  slags.

Due to the problem of hydration of the CaO in pure form, high grade  $CaCO_3$  was used as source of CaO. Calcination of the  $CaCO_3$  was performed at 1200°C for 5 hours in a muffle furnace, heated by silicon carbide heating elements, and using a Pt-crucible for containment of the powder. After calcination, the calcium oxide was cooled in a water free atmosphere by placing the Pt-crucible with the contents, still at 1200°C, directly into a desiccator. Only a few minutes was allowed between the subsequent crushing of the CaO pellet and the weighing of the powders, to prevent any changes occurring in the composition of the CaO.

The  $Al_2O_3$  powder was dried by heating at 800°C for 5 hours. Samples (typically 20g) were made up by weighing the required mass of powders on an electronic mass-balance, reporting the weight to the nearest milligram, and mixing these powders thoroughly in a swing mill for 5 minutes. After thorough mixing, the pellets (15mm diameter and 20mm in height) were pressed and sintered for 3 hours at 1200°C, crushed and re-mixed. This was followed by another pelletizing and sintering cycle. According to need, pieces of 0.2g were chipped from the pellet and enriched with vanadium by adding pre-determined amounts of  $V_2O_5$  or metallic vanadium powder (particle size: 5 $\mu$ m) to the chunks. The chunks with the vanadium additions were thoroughly mixed in a swing mill before charging into the vanadium crucible. The mixed powder was compacted to ensure the maximum amount of reagents to be present within the crucible. The crucible was filled to

just below the first groove, which was machined into the inner wall. The slag depth in the crucible after melting was about 2.5 mm, yielding a slag mass of ca. 0.2g.

### **2.3.2. Experimental run.**

The crucible containing the slag was introduced cold to the furnace, then heated at 2°C/min to 1400°C under purified argon. The gas stream was switched to the hydrogen-water mixture at 1400°C. Subsequent heating to the equilibration temperature was at 1°C/min holding the sample at this final temperature for 6 hours before quenching. Some minutes before quenching the hydrogen-water mixture was replaced by purified Argon for safety reasons. After quenching the sample was retrieved from the water, and the perforated PVC membrane was replaced with a new layer of PVC with the furnace still at the equilibration temperature. Oxidation of molybdenum occurs even in deoxygenated Argon at 1700°C. Hence, after the replacement of the PVC membrane the Argon was again replaced by hydrogen, for the duration of the cooling cycle. Prior to opening, the furnace was once more flushed with Argon. The thick Molybdenum wires lasted for 5 equilibration cycles before needing replacement.

### **2.3.3. Sample analysis**

After being retrieved from the water the crucible with slag was dried for 10 minutes at 100°C. The crucible was mounted in an epoxy resin (impregnated under vacuum). Polymerization of the resin was performed at 90°C for 4 hours. Following polymerization, the crucible was sectioned along its axis using a diamond cut-off wheel. Despite using a diamond cut-off wheel, it still took half an hour to cut through the supposedly pure vanadium crucible.

From the XRD-pattern, shown in Figure 40, the presence of vanadium nitride phases are identified in the vanadium crucible after equilibration.

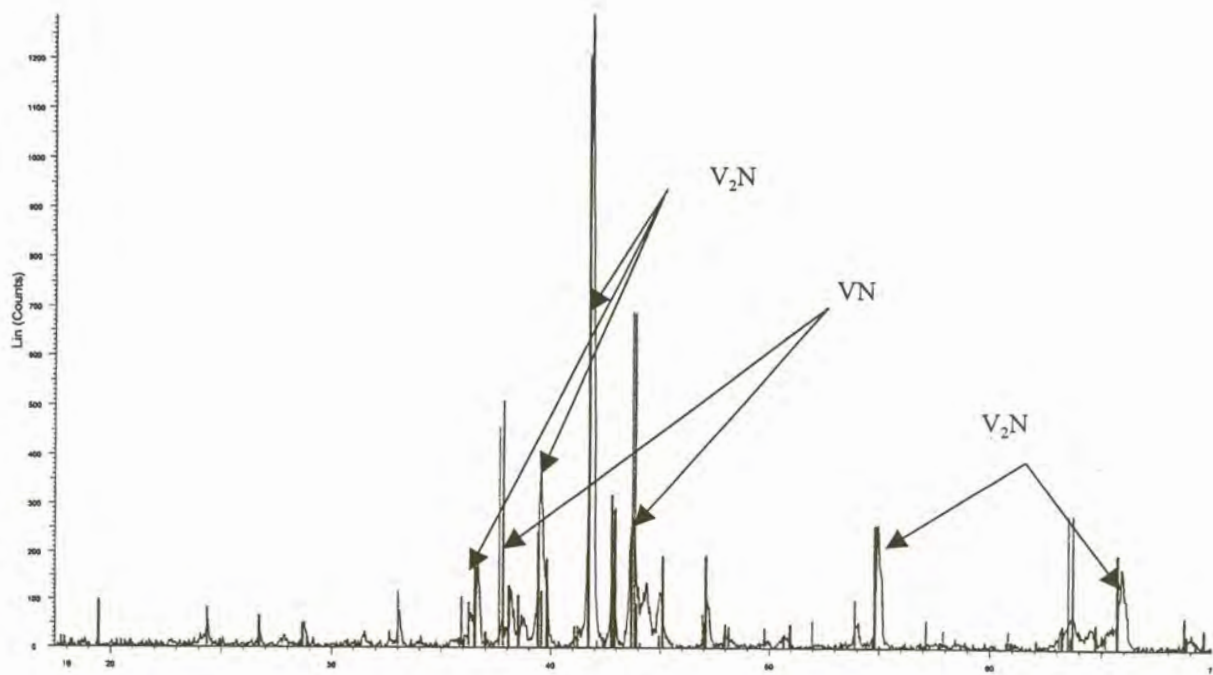


Figure 40: XRD-pattern of vanadium crucible after equilibration.

Vanadium readily reacts with nitrogen, most probably an impurity in the Argon, at 1700°C to give rise to the vanadium nitride phases. These vanadium nitride phases are extremely hard and show great cutting resistance. The sectioned vanadium crucible was subsequently polished down to 3 microns using diamond paste. Following polishing, the crucible was coated with a thin layer of carbon before chemically analysed by energy dispersive x-ray analysis (EDX) using a Joel 5800 Electron microscope with a microanalyser. Other bulk chemical analysis techniques could not be used, since the slag, specially low basicity slags, contained vanadium metal particles (whether as a result of partial reduction of the vanadium oxide which had been added as  $V_2O_5$  to the slag mixture, or of unreacted vanadium metal powder). Entrained vanadium metal particles are shown in figure 41.

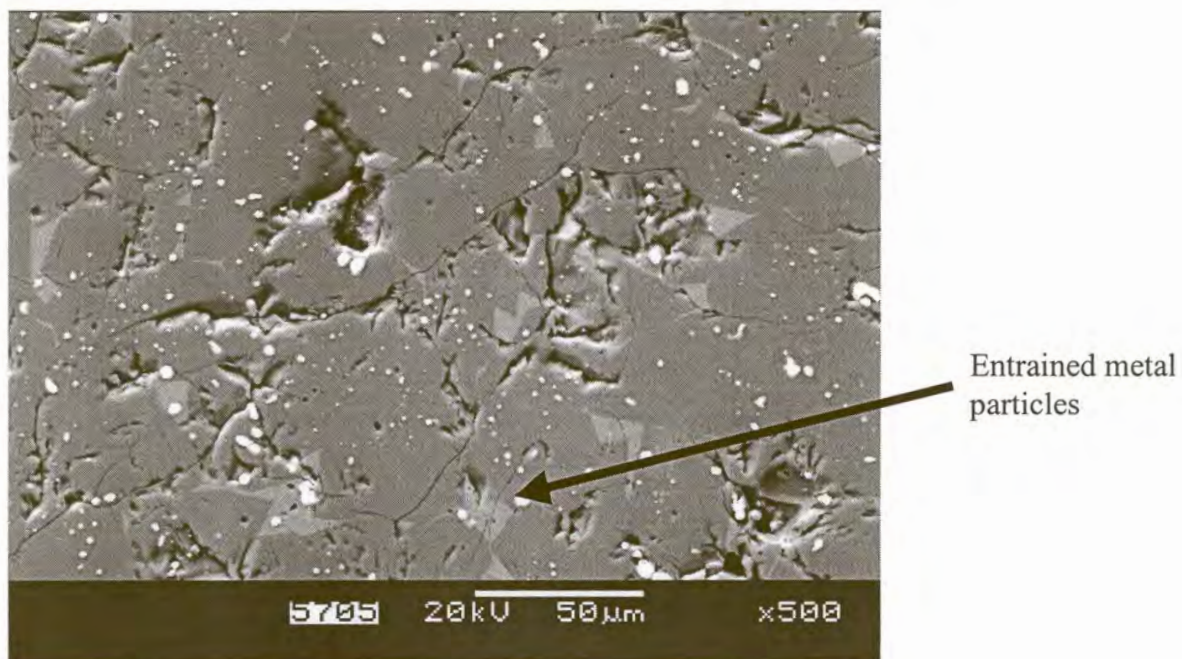


Figure 41: Back-scattered electron image of equilibrated slag sample showing entrained metal particles.

By examining the sample with back-scattered electron imaging, such metal particles were readily discerned, and avoided during EDX analysis. The analyses were performed using 20 kV acceleration voltage at a working distance of 10mm, using 100 seconds of analysis time. A total of 30 fields was typically analysed per sample, using this set of analyses to calculate the 95% confidence intervals on the average  $\text{CaO}:\text{Al}_2\text{O}_3$  ratio, and average mole fraction of vanadium.

The solidified slag typically contained two or more crystalline phase, and care was taken to ensure representative sampling of all the phases. Figure 42 and 43 depict cases where more than two crystalline phases were identified.

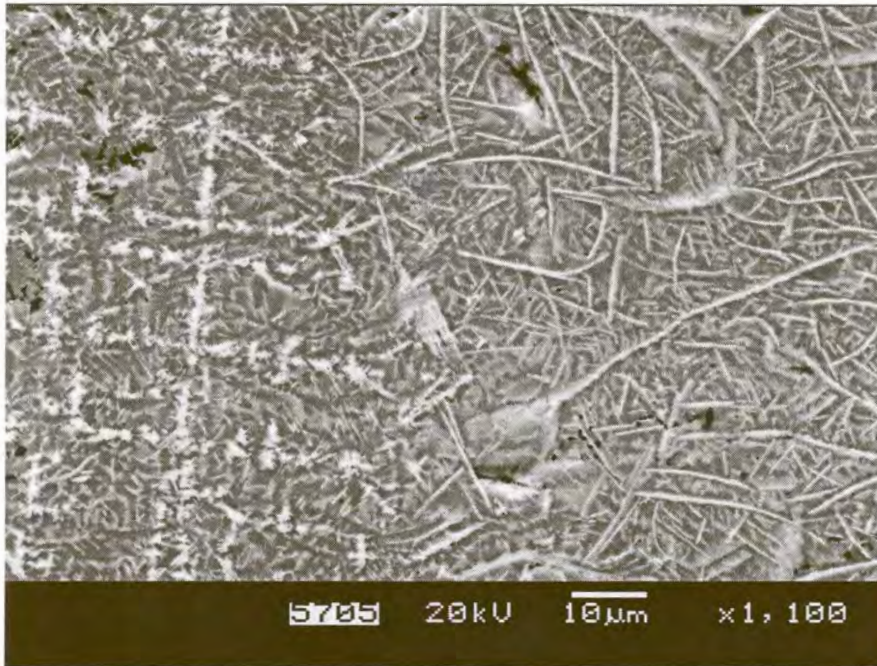


Figure 42: Back-scattered electron image of slag 7 after equilibration, showing more than two crystalline phases.

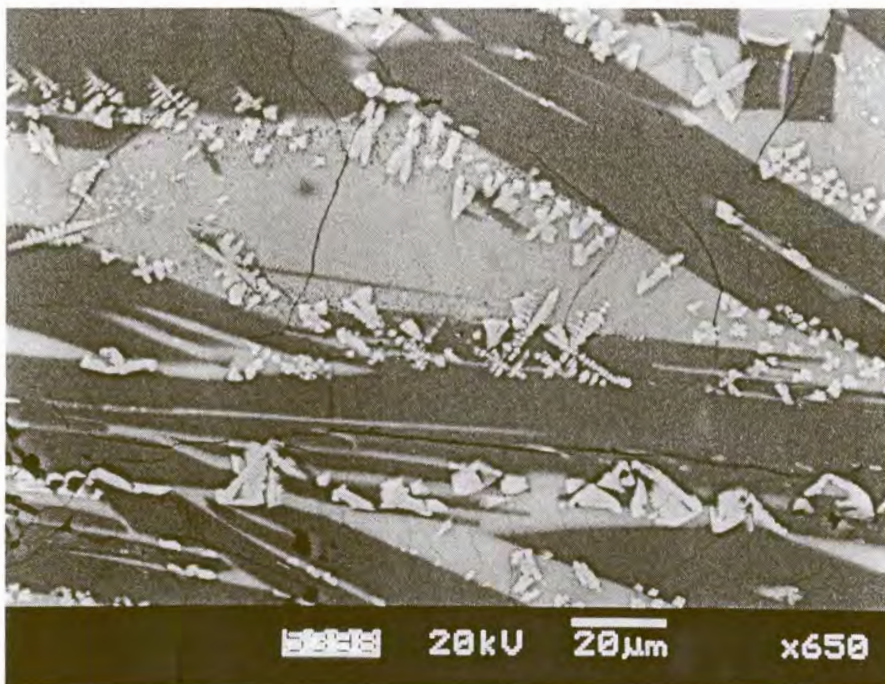


Figure 43: Back-scattered electron image of slag 5 after equilibration, showing more than two crystalline phases.

A combination of relatively slow cooling, due to the water vapour cloud surrounding the crucible during quenching, and the phase stabilizing effect of vanadium on the high basicity slags ( $\text{CaO}:\text{Al}_2\text{O}_3 > 0.7$ ) gave rise to formation of multiple crystalline phases. The high basicity slags ( $\text{CaO}:\text{Al}_2\text{O}_3 > 0.7$ ) usually did not contain any entrained vanadium metal particles.